Coupling of ferroelasticity and ferromagnetism in $La_{1-x}Sr_xCoO_3$ twin crystals

Tôru Kyômen,[1,*] Akito Sano,[1] Yohei Murachi,[1] Minoru Hanaya,[1] Kosuke Suzuki,[2] and Masahisa Ito[2]
[1]*Graduate School of Engineering, Department of Chemistry and Chemical Biology, Gunma University, Tenjin-cho 1-5-1, Kiryu 376-8515, Japan*
[2]*Graduate School of Engineering, Department of Electronic Engineering, Gunma University, Tenjin-cho 1-5-1, Kiryu 376-8515, Japan*
(Received 19 April 2010; revised manuscript received 17 June 2010; published 3 August 2010)

In the present study, x-ray diffraction experiments under magnetic fields were carried out for $La_{0.57}Sr_{0.44}CoO_{3.01}$ twin crystals with a trigonal structure by Laue method in addition to magnetization measurements. Crystallographic domains (variants) in a ferromagnetic phase of the crystals were rearranged by applying magnetic fields and the rearranged structure remained even after the applied magnetic fields were changed to zero, indicating a coupling of ferroelasticity and ferromagnetism. The present results were consistently understood by the large uniaxial magnetocrystalline anisotropy with an easy plane of magnetization parallel to the hexagonal *ab* plane of the trigonal structure. The origin of the large magnetocrystalline anisotropy was discussed in relation to the spin states of Co ions.

DOI: 10.1103/PhysRevB.82.064402 PACS number(s): 75.80.+q, 62.20.fg, 75.30.Gw, 75.60.Ej

I. INTRODUCTION

In recent years, ferromagnetic shape memory alloys have attracted many researchers because of their technological importance and interesting physical properties.[1–3] In these alloys, crystallographic domains (variants) in ferromagnetic martensite phases are rearranged by external magnetic fields due to the large magnetocrystalline anisotropy resulting in huge magnetostrictions with several percent. This is a result of a coupling of ferroelasticity and ferromagnetism. Because this mechanism is not limited to alloys, such a function would be present in other ferromagnetic materials such as oxides.

$La_{1-x}Sr_xCoO_3$ crystals have a cubic perovskite-type structure (space group: $Pm3m$), as shown in Fig. 1, at high temperatures. The crystals ($0 \leq x \leq 0.5$) show a structural phase transition from the cubic structure to a trigonal structure (space group: $R\bar{3}c$) at a certain temperature which decreases from about 1600 to 400 K with increasing x from 0 to 0.5.[4] In the phase transition, CoO_6 octahedra are rotated about an axis parallel to one of $\langle 111 \rangle$ directions of the cubic lattice accompanied by contraction along the axis. The crystallographic directions or planes are indexed by the (pseudo-) cubic lattice in this paper. Relation between the cubic lattice and the hexagonal lattice of the trigonal structure is shown in Fig. 1. The hexagonal c_h and a_h axes correspond to $\langle 111 \rangle$ and $\langle 110 \rangle$ directions of the cubic lattice, respectively. There are thus four possibilities to choice the direction of c_h axis, i.e., $[111]$, $[\bar{1}11]$, $[1\bar{1}1]$, and $[11\bar{1}]$, when the crystal transforms from the cubic to the trigonal phases. Therefore, the crystal has multidomain structure (twin structure) composed of four variants in the trigonal phase and these variants meet on the pseudocubic {100} or {110} plane according to literature.[4–7] In addition, ferroelastic properties have been reported in the trigonal phase of $LaCoO_3$ crystal.[8,9] Such a ferroelasticity is expected to be present also in Sr-doped $LaCoO_3$ crystals of $La_{1-x}Sr_xCoO_3$ having the same crystal structure as $LaCoO_3$.

$La_{1-x}Sr_xCoO_3$ ($x \geq 0.3$) crystals show a ferromagnetic phase transition below 200–250 K.[10–15] In our previous paper,[15] we have reported that the crystal with the trigonal structure was easily magnetized when a magnetic field was applied parallel to $\langle 110 \rangle$ directions of the pseudocubic lattice but hardly magnetized when a magnetic field was applied parallel to $\langle 100 \rangle$ directions of the pseudocubic lattice. Based on these results, we have proposed that this crystal has large uniaxial magnetocrystalline anisotropy with an easy plane of magnetization parallel to the hexagonal *ab* plane (see Fig. 1). The coexistence of large magnetocrystalline anisotropy and ferroelasticity expected in $La_{1-x}Sr_xCoO_3$ crystals may induce a coupling of ferroelasticity and ferromagnetism. In fact, Ibbara *et al.*[15] have reported a sign of the coupling: a huge anisotropic magnetostriction has been observed in $La_{1-x}Sr_xCoO_3$ polycrystals which were stretched parallel to an external magnetic field direction and compressed perpendicular to the direction.

In the present study, x-ray diffraction experiments under magnetic fields were carried out for $La_{0.57}Sr_{0.44}CoO_{3.01}$ twin

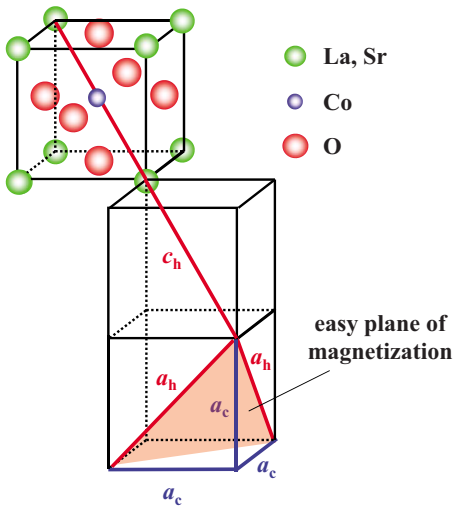

FIG. 1. (Color online) Relation between the (pseudo-) cubic lattice and the hexagonal lattice of the trigonal structure of $La_{1-x}Sr_xCoO_3$ crystals. Lines indicated by a_c's are edges of the cubic unit cell. Lines indicated by a_h's and c_h are edges of the hexagonal unit cell. A triangle plane is an easy plane of magnetization parallel to the *ab* plane of the hexagonal lattice expected from the magnetization measurements (Ref. 15).

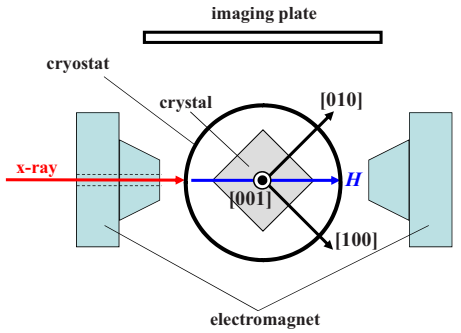

FIG. 2. (Color online) Configuration of a crystal, cryostat, electromagnet, imaging plate, and incident x-ray direction when Laue photographs were taken in the present study.

crystals by Laue method in addition to magnetization measurements. The results showed that variants of the crystals in a ferromagnetic phase were rearranged by applying magnetic fields and that the rearranged structure remained even after the applied magnetic field was changed to 0 Oe, indicating a coupling of ferroelasticity and ferromagnetism originating from large magnetocrystalline anisotropy. The origin of the large magnetocrystalline anisotropy was discussed in relation to the spin states of Co ions.

II. EXPERIMENTAL DETAILS

$La_{0.57}Sr_{0.44}CoO_{3.01}$ single crystals grown by a flux method[15] were used for the present studies. The crystals have the trigonal structure (a=0.5410 nm, α=60.27° in rhombohedral lattice), the crystal shape is close to a cube with edge length of about 0.1 mm, the edges are parallel to ⟨100⟩ directions of the pseudocubic lattice, and the Curie temperature is about 250 K.[15] Magnetizations of the single crystals were measured using a superconducting quantum interference magnetometer (MPMS-5SW, Quantum Design). In the measurements, one crystal was fixed on a plastic plate by resin and inserted into a sample holder (plastic straw). Magnetization of the resin was ignorable. X-ray diffraction studies under magnetic fields by Laue method were carried out at the station BL-3C of the synchrotron-radiation facility, Photon Factory, in Tsukuba, Japan.[16] Fig. 2 shows the configuration of a crystal, electromagnet, cryostat, imaging plate, and incident x-ray direction when Laue photographs were taken. Orthogonal coordinate axes on the crystal are defined parallel to the edges of the pseudocubic lattice as shown in the figure. White x-rays emitted from a bending magnet of the storage ring were used as the incident x-rays. Size of the incident x-ray was controlled to 0.1 mm square by using a slit to make the x-ray beam size same as the sample size. The incident x-rays parallel to the [110] direction were irradiated to the sample for about 1 s through a hole of the magnet. The sample position was controlled for the whole incident x-ray beam to be irradiated to the sample by monitoring intensity of fluorescent x-rays of Sr $K\alpha$ (14.17 keV) with an energy-dispersive germanium detector. A normal line of the imaging plate was set perpendicular both to the incident x-ray direction and to the [001] direction. The sample was cooled in a

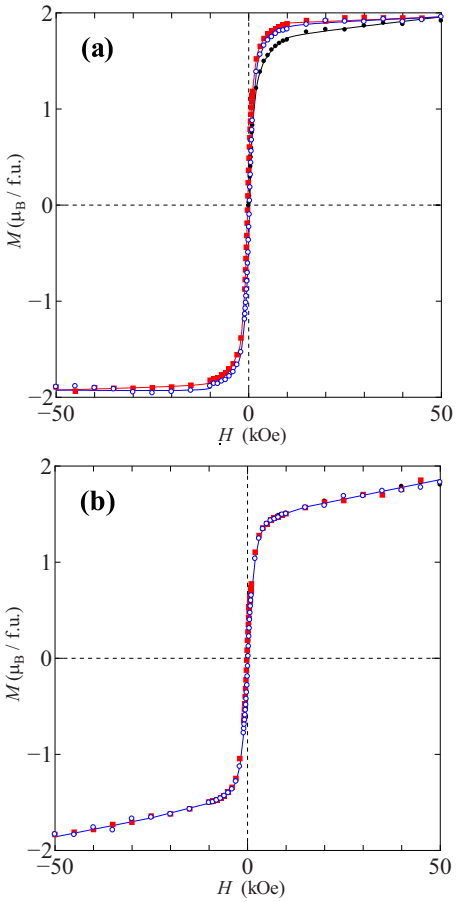

FIG. 3. (Color online) MH hysteresis curve of $La_{0.57}Sr_{0.44}CoO_{3.01}$ twin crystals when magnetic fields were applied at 4 K parallel to (a) the [110] and (b) the [100] directions of the pseudocubic lattice. Solid circles, solid squares, and open circles are results obtained by successive scans from 0 kOe to 50 kOe, from 50 kOe to −50 kOe, and from −50 kOe to 50 kOe, respectively. Solid lines are guide for eyes.

cryostat under 0 Oe from room temperature to 30 K before Laue photographs were taken at 30 K. Magnetic fields can be applied along the [110] direction with the configuration shown in Fig. 2. In addition, magnetic fields were applied parallel to $[1\bar{1}0]$ and [100] directions as follows. The crystal can be rotated about the [001] axis. The crystal was rotated by 90° about the [001] axis when a magnetic field was applied parallel to the $[1\bar{1}0]$ direction. The crystal was rotated by 45° about the [001] axis when a magnetic field was applied parallel to the [100] direction. In these cases, Laue photographs were taken after the applied magnetic field was changed to 0 Oe by turning off the electromagnet and then the crystal was returned to the initial orientation shown in Fig. 2.

III. RESULTS

Figure 3(a) shows MH hysteresis curve of $La_{0.57}Sr_{0.44}CoO_{3.01}$ as-prepared crystal when magnetic fields were applied parallel to the [110] direction of the pseudocu-

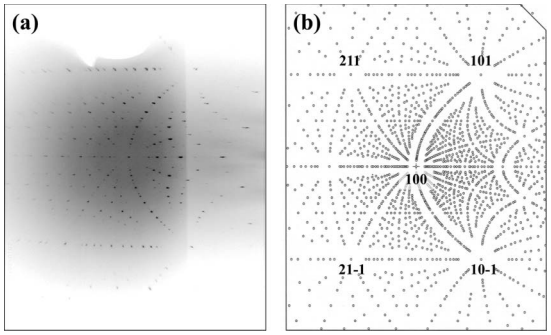

FIG. 4. Laue photograph of $La_{0.57}Sr_{0.44}CoO_{3.01}$ twin crystals obtained at (a) room temperature and under zero magnetic field and (b) the simulation pattern assuming a simple cubic cell.

bic lattice after cooling to 4 K under 0 Oe. This *MH* hysteresis curve showed an anomalous behavior that the magnetizations of the initial scan from 0 to 50 kOe (solid circles in the figure) were smaller than those of the scan from −50 kOe to 50 kOe (open circles) at a same field. After this measurements, the sample was taken out from the magnetometer, orientation of the crystal was changed so that magnetic fields can be applied parallel to a [100] direction, and then *MH* hysteresis curves were measured along the [100] direction after zero-field cooling to 4 K. Figure 3(b) shows the *MH* hysteresis curve. This *MH* curve showed no anomalous behavior contrary to that along the [110] direction as shown in Fig. 3(a). By using another as-prepared crystal, *MH* hysteresis curves were also measured with changing the order of the directions of applying magnetic fields, namely, *MH* hysteresis curve was measured at first along a [100] direction and then along a [110] direction. No change was observed with the order of the directions and the same results as shown in Figs. 3(a) and 3(b) were obtained. These behaviors were observed even at 230 K just below the Curie temperature of ~250 K.

Figure 4(a) shows Laue photograph of $La_{0.57}Sr_{0.44}CoO_{3.01}$ as-prepared crystal taken at room temperature and under 0 Oe. The distance from the crystal to the imaging plate was set to be 5 cm. Figure 4(b) shows the simulation pattern obtained by assuming a simple cubic unit cell with a lattice constant $a=0.3833$ nm. The experimental Laue pattern was well reproduced by the simulation. However, each Laue spot splits into some spots. This indicates that the crystal has multidomain structure at room temperature. Laue photographs were taken also using other $La_{0.57}Sr_{0.44}CoO_{3.01}$ crystals. Although the details of splitting patterns of Laue spots were different for every crystal, the following results were qualitatively the same each other.

Figures 5 and 6 show Laue photographs around a 100 diffraction spot taken at 30 K. All the photographs were taken in the same configuration as shown in Fig. 2. The distance from the crystal to the imaging plate was set to be 18 cm. The insets are enlarged figures of the 100 diffraction spot. The photograph of Fig. 5(a) was taken just after the sample was cooled under 0 Oe from room temperature to 30 K. It is found that each pseudocubic Laue spot splits into several spots due to multidomain structure. After that, 20 kOe was applied parallel to the [110] direction and then the

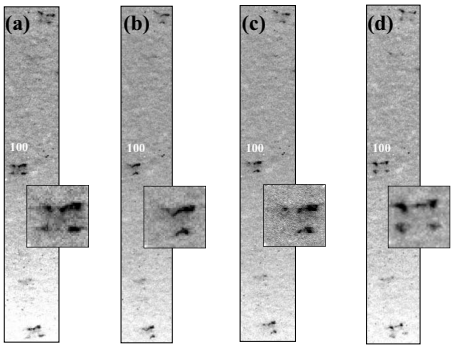

FIG. 5. Laue photographs of $La_{0.57}Sr_{0.44}CoO_{3.01}$ twin crystals around a 100 diffraction spot taken at 30 K. The insets are enlarged figures of the 100 diffraction spot: (a) just after zero field cooling, (b) under 20 kOe parallel to the [110] direction of the pseudocubic lattice, (c) after changing the applied magnetic field to 0 Oe, and (d) after applying 20 kOe parallel to the $[1\bar{1}0]$ direction of the pseudocubic lattice for 5 min and then changing the applied magnetic field to 0 Oe. See text for details.

photograph of Fig. 5(b) was taken under 20 kOe. Left-bottom spots split from each pseudocubic spot disappeared and the left-upper spots were weakened in comparison with the right-side spots. Then, the magnetic field was changed to 0 Oe by turning off the electromagnet and the photograph of Fig. 5(c) was taken under 0 Oe. No remarkable difference was observed between Figs. 5(b) and 5(c). Then, the crystal was rotated by 90° about the [001] axis and 20 kOe was applied parallel to the $[1\bar{1}0]$ direction for 5 min. After the magnetic field was changed to 0 Oe and the crystal was returned to the initial orientation, the photograph of Fig. 5(d) was taken under 0 Oe. The left-bottom spots appeared again, the left-upper spots were intensified, and the right-side spots were weakened.

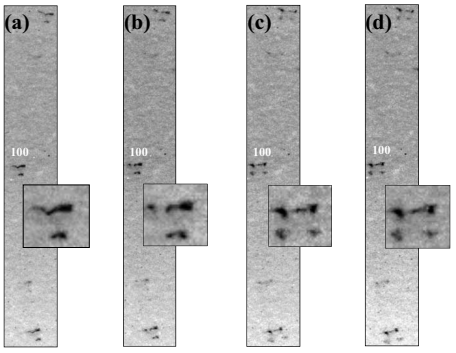

FIG. 6. Laue photographs of $La_{0.57}Sr_{0.44}CoO_{3.01}$ twin crystals around a 100 diffraction spot taken at 30 K. The insets are enlarged figures of the 100 diffraction spot: (a) after applying 20 kOe parallel to the [110] direction of the pseudocubic lattice for 5 min and then changing the applied magnetic field to 0 Oe, (b) after applying 20 kOe parallel to the [100] direction of the pseudocubic lattice and then changing the applied magnetic field to 0 Oe, (c) after applying 20 kOe parallel to the $[1\bar{1}0]$ direction of the pseudocubic lattice for 5 min and then changing the applied magnetic field to 0 Oe, and (d) after applying 20 kOe parallel to the [100] direction of the pseudocubic lattice and then changing the applied magnetic field to 0 Oe. See text for details.

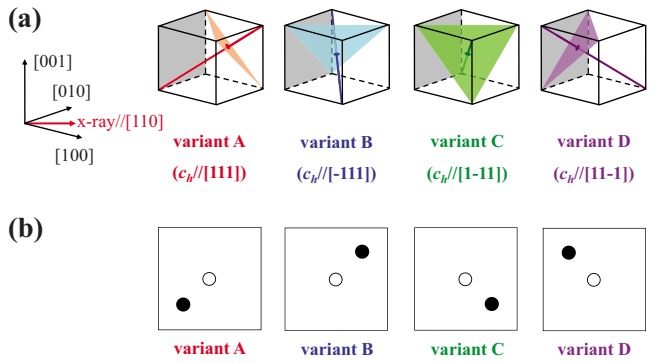

FIG. 7. (Color online) (a) Schematic drawing of four variants in $La_{1-x}Sr_xCoO_3$ crystals. Cubes, lines parallel to the body diagonal, and triangle planes represent the cubic lattices, the c_h axes, and the easy planes of magnetization, respectively, for the respective variants. The coordinate axes of the cubic lattices are shown in the left side. X-rays were irradiated parallel to the [110] direction as indicated by an arrow. Hatched parallelogram planes indicate (100) planes. (b) Relative positions of the 100 diffraction spots on the imaging plate expected for cubic (open circles) and trigonal (solid circles) phases.

After the above experiments, 20 kOe was applied again parallel to the [110] direction for 5 min. After the magnetic field was changed to 0 Oe, the photograph of Fig. 6(a) was taken under 0 Oe. The photograph of Fig. 6(a) was similar to the photograph of Fig. 5(c). Then, the crystal was rotated by 45° about the [001] axis and 20 kOe was applied parallel to the [100] direction for 5 min. After the magnetic field was changed to 0 Oe and the crystal was returned to the initial orientation, the photograph of Fig. 6(b) was taken under 0 Oe. There is no remarkable difference between Figs. 6(a) and 6(b). Then, the crystal was rotated by 90° about the [001] axis and 20 kOe was applied parallel to the $[1\bar{1}0]$ direction for 5 min. After the magnetic field was changed to 0 Oe and the crystal was returned to the initial orientation, the photograph of Fig. 6(c) was taken under 0 Oe. The change from Fig. 6(b) to Fig. 6(c) was similar to that from Fig. 5(c) to Fig. 5(d). Then, the crystal was rotated by 45° about the [001] axis and 20 kOe was applied parallel to the [100] direction for 5 min. After the magnetic field was changed to 0 Oe and the crystal was returned to the initial orientation, the photograph of Fig. 6(d) was taken under 0 Oe. There is also no remarkable difference between Figs. 6(c) and 6(d).

IV. DISCUSSION

The peculiar behavior of $La_{0.57}Sr_{0.44}CoO_{3.01}$ crystals described above and shown in Figs. 3, 5, and 6 is understood as a result of the ferroelasticity-ferromagnetism coupling as follows. As mentioned in Introduction, this crystal has multidomain structure composed of four variants with different directions of c_h axes. Figure 7(a) shows a schematic drawing of the four variants A, B, C, and D. Cubes, lines parallel to a body diagonal, and triangle planes in the figure represent the cubic lattices, the c_h axes, and the easy planes of magnetization for the respective variants, respectively. Open and solid circles in Fig. 7(b) show relative positions of 100 diffraction spots in cubic and trigonal phases, respectively, for the respective variants, expected in the Laue photograph under the present instrumental setting shown in Fig. 2. For variant A, (100) planes of the cubic phase [e.g., hatched parallelogram area in Fig. 7(a)] tilt to the left-bottom direction in the trigonal phase because the crystal is compressed along the c_h axis parallel to the [111] direction. Then, the Laue spot shifts to the left-bottom side in the trigonal phase from the cubic position as shown in Fig. 7(b) because x-rays are irradiated parallel to the [110] direction as shown in Fig. 7(a). From the same consideration, 100 diffraction spots shift to the right-upper, right-bottom, and left-upper sides for variants B, C, and D, respectively, in the trigonal phase from the cubic positions. In fact, four spots were mainly observed in Figs. 5 and 6.

When a magnetic field is applied parallel to the [110] direction, the magnetic field is parallel to the easy planes of magnetization for variants B and C but is not for variants A and D. If the crystal were a soft ferromagnet, the magnetizations in variants A and D would rotate into the magnetic field direction in order to decrease the magnetocrystalline anisotropy energy. However, the magnetization cannot rotate easily in $La_{0.57}Sr_{0.44}CoO_{3.01}$ crystal because of the large magnetocrystalline anisotropy as found from Fig. 3. Instead, variants are rearranged because the crystal has ferroelasticity. Namely, variants A and D transform to variants B or C, possibly by migration of twin boundaries, resulting in that two left-side spots in Laue photograph are weakened and the two right-side spots are intensified. This was actually observed in Fig. 5(b). The relative intensities of these spots were not changed after the external magnetic field was changed to 0 Oe as shown in Fig. 5(c). This indicates that the rearranged variants do not return to the initial arrangement due to ferroelasticity. From the same consideration, when a magnetic field is applied parallel to the $[1\bar{1}0]$ direction, variants B and C should transform to variant A or D and then left-side spots should be intensified and the right-side spots should be weakened as was observed in Fig. 5(d). No rearrangement of variants should occur when a magnetic field is applied parallel to the [100] direction because the angles between the magnetic field and the easy planes of magnetization are same for four variants and thus the magnetocrystalline anisotropy energies are same for four variants. This is consistent with the results of Fig. 6.

The behavior of the *MH* hysteresis curves shown in Figs. 3(a) and 3(b) is also understood by the same consideration as discussed in the last paragraph. An anomalous *MH* hysteresis curve was observed along the [110] direction as shown in Fig. 3(a). In the initial field scan along the direction, the multidomain structure composed of variants A, B, C, and D gradually changes to a structure composed of only variants B and C with easy planes parallel to the applied magnetic fields. Thus, the magnetization is relatively small at low fields because the magnetic fields are not parallel to the easy planes of variants A and D. After the magnetic field was increased up to 50 kOe, the crystal becomes to be composed of only variants B and C and then the crystal is easily magnetized along the [110] direction in the successive scans from 50 to −50 kOe and −50 to 50 kOe. No anomalous *MH* hys-

teresis curve was observed along the [100] direction as shown in Fig. 3(b). This is also understood by considering that the angles between the magnetic field and the easy planes of magnetization are same for four variants.

Actually, the number of split spots was not exactly four and the splitting pattern was more complex. In addition, the splitting pattern was different for every crystal. These facts imply that the variants are connected to each other with complicated strains producing intermediate structures within the crystals besides the variants A–D.

As found from Fig. 3, coercive force of this crystal was small (about 200 Oe) in spite of the large magnetocrystalline anisotropy. Such a property has been observed also in polycrystalline samples whose magnetization does not saturate even at 50 kOe in spite of the small coercive force.[10,12] This is easily understood by considering that the magnetocrystalline anisotropy is absent or small within the easy plane of magnetization. In this case, ferromagnetic domain walls are created easily by rotating magnetic moments of Co ions within the easy plane and thus the ferromagnetic domain walls easily migrate by external magnetic fields.

Ibarra *et al.*[14] have reported a huge anisotropic magnetostriction in $La_{1-x}Sr_xCoO_3$ polycrystals. Their results were as follows. (1) The crystals were stretched parallel to an external magnetic field direction and compressed perpendicular to the direction. (2) The volume was not changed appreciably by external magnetic fields. (3) No appreciable magnetostriction occurred due to migration of ferromagnetic domain walls at low fields. These results are consistently understood as follows. By applying high magnetic fields to the polycrystalline samples, c_h axes of respective variants change to one of $\langle 111 \rangle$ directions so that the angle between the c_h direction and the magnetic field direction is closest to 90°, resulting in the contraction perpendicular to the magnetic field direction along with the stretching parallel to the direction. Because of the rearrangement of variants, the volume change is absent essentially. Since the migration of ferromagnetic domain wall occurs by rotating magnetic moments of Co ions within the easy plane of magnetization and the magnetocrystalline anisotropy is absent or small within the easy plane, a magnetostriction by the migration should be small as compared with that by rearrangement of variants.

It was found that the magnetocrystalline anisotropy is large in $La_{0.57}Sr_{0.44}CoO_{3.01}$ in spite of the small trigonal distortion that is found from a lattice parameter of the rhombohedral lattice; $\alpha=60.27°$ ($\alpha=60°$ in the cubic structure). The origin of the large magnetocrystalline anisotropy is discussed here in relation to spin states of Co ions based on a localized model of $3d$ electrons. $3d$ orbitals of Co ions in $La_{1-x}Sr_xCoO_3$ split into doubly degenerate e_g orbitals and triply degenerate t_{2g} orbitals when the crystal has the cubic structure. High ($t_{2g}^4e_g^2$), intermediate ($t_{2g}^5e_g^1$), and low (t_{2g}^6) spin states are possible for Co^{3+} ions.[10] High ($t_{2g}^3e_g^2$), intermediate ($t_{2g}^4e_g^1$), and low (t_{2g}^5) spin states are possible for Co^{4+} ions.[10] When the crystal has the trigonal structure, the $3d$ orbitals split into doubly degenerate e_2 orbitals, doubly degenerate e_1 orbitals, and nondegenerate a orbital, as shown in Fig. 8. According to magnetic circular x-ray dichroism studies of $La_{1-x}Sr_xCoO_3$, these compounds have finite orbital magnetic moments. Though orbital magnetic moments are present both in e_2 and e_1 orbitals that in e_2 orbitals is small when trigonal distortion is small. Because the trigonal distortion of $La_{0.57}Sr_{0.44}CoO_{3.01}$ is small, the orbital magnetic moment should originate from e_1 orbitals. Only Co^{3+} in the intermediate-spin state and Co^{4+} in the low-spin state, shown in Fig. 8, have the e_1 orbital magnetic moment because the electron configuration is e_1^3. Therefore, Co^{3+} in the intermediate-spin state or Co^{4+} in the low-spin state should be present in $La_{0.57}Sr_{0.44}CoO_{3.01}$. We propose from the following considerations that all Co^{3+} ions are in the intermediate-spin state and all Co^{4+} ions are in the low-spin state in $La_{0.57}Sr_{0.44}CoO_{3.01}$. In the proposed spin states, the spin magnetic moment is 1.57 μ_B per Co ion and the orbital magnetic moment is 0.43 μ_B per Co ion for $La_{0.57}Sr_{0.44}CoO_{3.01}$ because the saturated magnetic moment was about 2 μ_B per Co ion [see Fig. 3(a)]. This is consistent with the results of magnetic circular x-ray dichroism studies: The orbital magnetic moment was ~0.3 μ_B and the ratio of the orbital magnetic moment to the spin magnetic moment was ~0.27.[17] In addition, e_2 electrons would migrate easily from Co^{3+} to Co^{4+} ions in the proposed spin states because the electron configuration of e_1 and a orbitals are the same ($a^2e_1^3$) for both ions. This is consistent with the fact that $La_{0.57}Sr_{0.44}CoO_{3.01}$ has metallic electric conductivity with low resistivity. Thus, we propose that the large e_1 orbital magnetic moment is the origin of the large magnetocrystalline anisotropy in $La_{0.57}Sr_{0.44}CoO_{3.01}$ in spite of the small trigonal distortion.

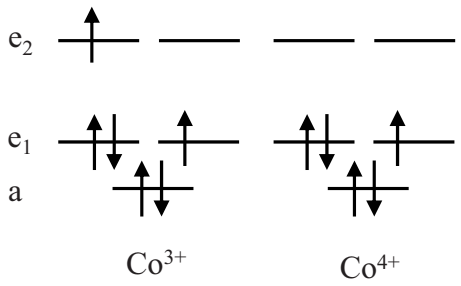

FIG. 8. Energy levels diagrams of Co ions in trigonal $La_{1-x}Sr_xCoO_3$ and proposed electron configurations of Co^{3+} and Co^{4+} ions in $La_{1-x}Sr_xCoO_3$.

V. CONCLUSION

In the present study, we succeeded in taking the Laue photographs of $La_{0.57}Sr_{0.44}CoO_{3.01}$ twin crystals even though the crystal size was only 0.1 mm. It was shown that crystallographic domains (variants) of $La_{1-x}Sr_xCoO_3$ in a ferromagnetic phase were rearranged by applying magnetic fields and that the rearranged structure remained after the applied magnetic fields were changed to 0 Oe. This indicates a coupling of ferroelasticity and ferromagnetism. In addition to the present results, other experimental facts such as a huge anisotropic magnetostriction reported by Ibarra *et al.*[14] were consistently understood by the large uniaxial magnetocrystalline anisotropy with an easy plane of magnetization parallel

to the hexagonal *ab* plane of the trigonal structure. We proposed that Co^{3+} ions are in the intermediate-spin state and Co^{4+} ions are in the low-spin state and that the large orbital magnetic moments in e_1 orbitals is the origin of the large magnetocrystalline anisotropy.

ACKNOWLEDGMENT

This work has been performed under the approval of the Photon Factory Program Advisory Committee (Proposal No. 2008G560).

*tkyomen@chem-bio.gunma-u.ac.jp

[1] K. Ullakko, J. K. Huang, C. Kantner, R. C. O'Handley, and V. V. Kokorin, Appl. Phys. Lett. **69**, 1966 (1996).
[2] Y. Sutou, Y. Imano, N. Koeda, T. Omori, R. Kainuma, K. Ishida, and K. Oikawa, Appl. Phys. Lett. **85**, 4358 (2004).
[3] R. Kainuma, Y. Imano, W. Ito, Y. Sutou, H. Morito, S. Okamoto, O. Kitakami, K. Oikawa, A. Fujita, T. Kanomata, and K. Ishida, Nature (London) **439**, 957 (2006).
[4] J. Mastin, M.-A. Einarsrud, and T. Grande, Chem. Mater. **18**, 6047 (2006).
[5] C. H. Kim, J. W. Jang, S. Y. Cho, I. T. Kim, and K. S. Hong, Physica B **262**, 438 (1999).
[6] C. H. Kim, S. Y. Cho, I. T. Kim, W. J. Cho, and K. S. Hong, Mater. Res. Bull. **36**, 1561 (2001).
[7] J. C. Walmsley, A. Bardal, K. Kleveland, M.-A. Einarsrud, and T. Grande, J. Mater. Sci. **35**, 4251 (2000).
[8] N. Orlovskaya, Y. Gogotsi, M. J. Reece, B. Cheng, and I. Gibson, Acta Mater. **50**, 715 (2002).
[9] M. Lugovy, V. Slyunyayev, N. Orlovskaya, D. Verbylo, and M. J. Reece, Phys. Rev. B **78**, 024107 (2008).
[10] M. A. Señarís-Rodríguez and J. B. Goodenough, J. Solid State Chem. **118**, 323 (1995).
[11] M. Itoh, M. Sugahara, I. Natori, and K. Motoya, J. Phys. Soc. Jpn. **64**, 3967 (1995).
[12] S. Chaudhary, S. B. Roy, and P. Chaddah, J. Alloys Compd. **326**, 112 (2001).
[13] S. Tsubouchi, T. Kyômen, and M. Itoh, Phys. Rev. B **67**, 094437 (2003).
[14] M. R. Ibarra, R. Mahendiran, C. Marquina, B. Garcia-Landa, and J. Blasco, Phys. Rev. B **57**, R3217 (1998).
[15] T. Kyômen, Y. Murachi, M. Itoh, and M. Hanaya, Chem. Mater. **20**, 5114 (2008).
[16] K. Suzuki, M. Ito, N. Tsuji, H. Adachi, and H. Kawata, Jpn. J. Appl. Phys. **48**, 056506 (2009).
[17] J. Okamoto, H. Miyauchi, T. Sekine, T. Shidara, T. Koide, K. Amemiya, A. Fujimori, T. Saitoh, A. Tanaka, Y. Takeda, and M. Takano, Phys. Rev. B **62**, 4455 (2000).